

ADHESIVE PRESSURE AS FAILURE CRITERION IN MICROMECHANICAL TESTS

Serge Zhandarov, Elena Pisanova, and Konrad Schneider

*Institute of Polymer Research
Hohe Str. 6, Dresden 01069, Germany*

SUMMARY: A new stress-based criterion of interfacial failure in micromechanical tests — critical interfacial normal stress, or *adhesive pressure* — is proposed. The new criterion has two important advantages: it follows the actual mechanism of crack initiation (in tensile Mode I) and allows to relate interfacial strength to such fundamental physical quantity as thermodynamic work of adhesion. The adhesive pressure values have been experimentally determined for several polymer/fiber model composites; it appeared to linearly depend on the work of adhesion measured independently. The model based on splitting the work of adhesion into the dispersion and acid-base contributions describes the observed relationships.

KEYWORDS: micromechanical tests, failure criteria, crack propagation, direct observation, adhesive pressure, work of adhesion, polymer matrices, reinforcing fibers.

INTRODUCTION

The quality of interfacial bonding in fibrous composites is traditionally characterized using micromechanical testing techniques, such as pull-out, microbond, micro-indentation. The normal practice is to measure the force, F , required to debond the fiber from the matrix, and then to calculate the mean (apparent) interfacial shear strength as the ratio of this maximum force to the embedded area:

$$\tau_{app} = \frac{F}{\pi d l_e},$$

where d is the fiber diameter, and l_e is the embedded length.

However, this approach is a gross oversimplification. In real test specimens, mechanical stress distribution has a very complicated pattern. The specimen fails, as a rule, by local "unzipping", or interfacial crack propagation, rather than through simultaneous shear over the whole embedded area. As was shown by recent research, the maximum force, F , measured in micromechanical tests, does not characterize the onset of debonding but corresponds to the start of unstable crack propagation, and its value is substantially influenced by friction in debonded regions.

Thus, existing micromechanical tests should be modified in two directions. First, the force corresponding to the start of debonding, F_d , should be measured; and second, relevant adhesion parameters should be deduced from the test data. It is obvious that the failure criterion should be local, i.e. refer to interfacial debonding at a given point rather than on the

average over the whole interface. In recent years, two such criteria for micromechanical tests have been proposed: ultimate interfacial shear strength, τ_{ult} , [1–3] and critical energy release rate, G_{ic} [1, 4]. The τ_{ult} and G_{ic} values calculated for different fiber/matrix interfaces provide

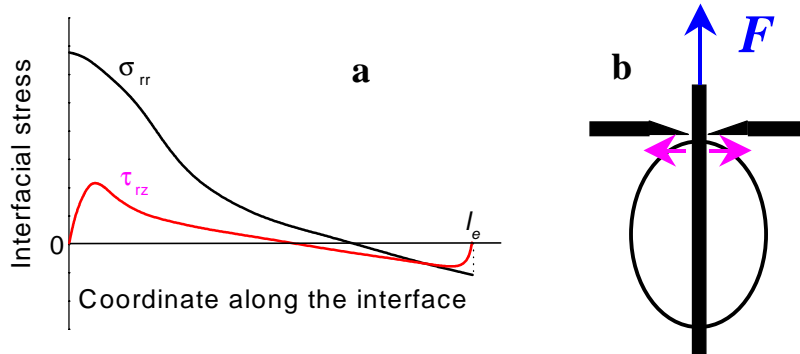


Fig. 1: Radial (σ_{rr}) and shear (τ_{rz}) interfacial stress distribution along the embedded length (a), and schematic view of the microbond test (b)

valuable information on interfacial bond strength; they appeared to be very sensitive to various fiber surface treatments and to the nature of the matrix. Nevertheless, in spite of their evident advantages as against old approaches, these new criteria cannot be regarded as adequate characteristics of adhesive interaction. Attempts to compare their values obtained by different researchers and/or by different techniques ran into difficulties; moreover, it was repeatedly noted that the calculated interfacial shear strength (IFSS) values appeared to be several times greater than the shear strength of the matrix. In all probability, it is due to the use of inadequate models of the debonding process. All existing approaches to τ_{ult} and G_{ic} estimation were based on the assumption that the interface fails in shear. This appeared to be obvious, but recent research has shown that it is not the case.

NORMAL INTERFACIAL STRESS AND ADHESIVE PRESSURE

In 1995, Scheer and Nairn [5] have published a paper in which presented, in particular, a variational mechanics analysis of the stresses in a loaded microbond specimen. According to their results, the interfacial shear stress, τ_{rz} , at the point of fiber entry into the matrix, is *zero* during the whole loading process until debonding starts, whereas the normal stress component, σ_{rr} , is at its maximum at this point (Fig. 1, a) and increases with external load. Thus, the start of debonding (crack initiation) at the point where the fiber enters the matrix occurs in normal tension (Mode I), as schematically represented in Fig. 1, b.

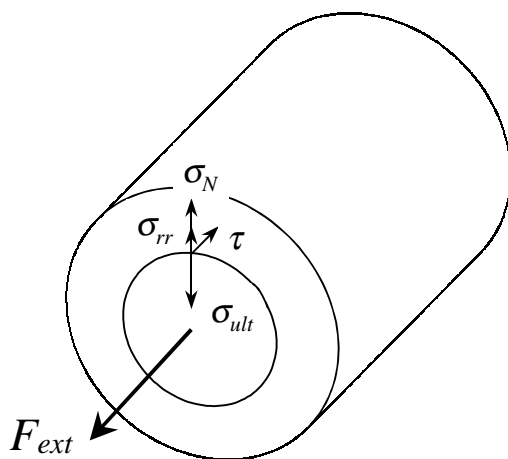


Fig. 2: Forces applied to the fiber and acting at the fiber/matrix interface

A similar result has been obtained by Marotzke [6] who used finite element modeling: at the moment of crack initiation, the failure mode was pure Mode I, and only with further crack propagation it changed to the mixed mode (I + II) reported by many researchers for the microbond test. Models based on tensile interfacial failure were also proposed by other researchers, e.g. Piggott [7]. It is natural to take the *critical normal stress*, or the maximum interfacial tensile stress value at which debonding starts from the fiber entry point, as a *new stress-based criterion of*

interfacial failure in the microbond test. Obviously, this value is numerically equal to the *adhesive pressure*, i.e., interfacial normal stress produced by molecular interaction between the fiber surface and the matrix. In more detail, the physical meaning of the new criterion can be seen in Fig. 2. Adhesive pressure at the interface, σ_{ult} , is balanced by the normal reaction of the fiber, σ_N , and the radial stress, σ_{rr} , acting from the matrix. With the increase of external load, F_{ext} , σ_{rr} increases and σ_N decreases, so as at any moment $\sigma_{rr} + \sigma_N = \sigma_{ult}$. When σ_N decreases to zero ($\sigma_{rr} = \sigma_{ult}$) and $F_{ext} = F_d$, debonding starts.

Adhesive pressure, as interfacial parameter, has yet another important advantage. The *work of adhesion* at the separation of two surfaces is done against this adhesive pressure; this allows to relate mechanical (strength) properties of adhesive joints to fundamental thermodynamic quantities and understand that it is adhesion that to a considerable extent determines strength of composite materials.

The term "adhesive pressure" for the normal stress, against which the work of adhesion is done, was introduced by Nardin and Schultz [8]. However, they did not propose any way to calculate σ_{ult} ; this has been done by Scheer and Nairn [5] who, in turn, did neither use σ_{ult} as a failure criterion nor relate it to the thermodynamic work of adhesion.

ADHESIVE PRESSURE AND WORK OF ADHESION

From the viewpoint of thermodynamics, adhesive interaction is specified by the reversible work of adhesion, W_A , needed to break a unit area of an adhesive contact. A direct measurement of the work of adhesion between two solids is only possible by using complicated experimental equipment (e.g., a surface force apparatus) and for particular specimen geometry (two spheres or two crossed cylinders). Therefore, the work of adhesion in fibrous composites is usually estimated indirectly, e.g., using the concept of acid-base

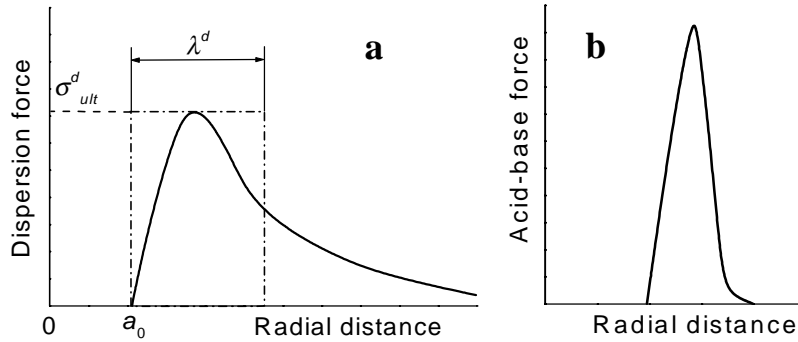


Fig. 3: Dispersion (a) and acid-base (b) force at the fiber/matrix interface as a function of radial separation

interactions and determining the donor and acceptor surface parameters by means of inverse gas chromatography (IGC) or flow sorption calorimetry. The estimated W_A values are typically by 2–3 orders of magnitude less than G_{ic} . For this reason, it was believed to recent times that there is no possibility to obtain the work of adhesion from micromechanical tests. At the same time, experimental investigations [9, 10] revealed a correlation between thermodynamic parameters of interacting materials and the bond strength. We have developed a model which relates the thermodynamic work of adhesion between a fiber and a matrix and the interfacial strength estimated from micromechanical tests.

The work of adhesion is done against normal stresses at the interface, i.e., in the case of fiber/matrix system, radial interfacial pressure, σ_{rr} , and can be expressed as

$$W_A = \int_{a_0}^{\infty} \sigma_{rr}(s) ds, \quad (1)$$

where s is the normal separation between the matrix and the fiber, and a_0 is its equilibrium value at zero external load.

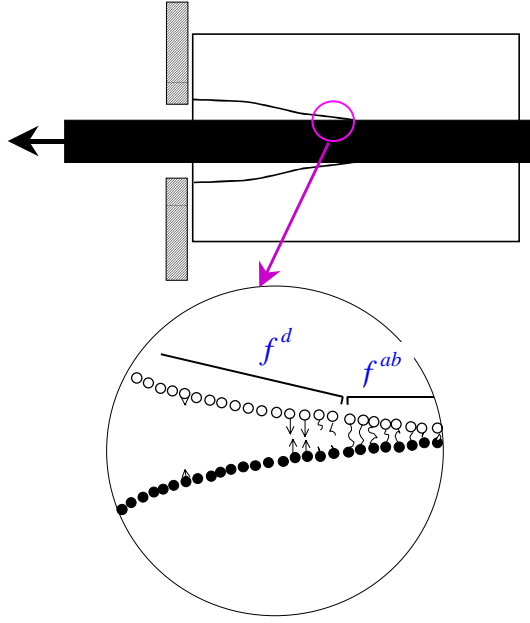


Fig. 4: Two types of molecular forces in an interfacial crack

When an adhesive contact fails, the local donor-acceptor (acid-base) bonds break first, and then, as the crack edges are being separated from each other, the dispersion interaction also gradually vanishes.

Fowkes [11] suggested that the dispersion and acid-base interactions can be considered as additive. It means that we can represent σ_{rr} as the sum of two contributions,

$$\sigma_{rr}(s) = \sigma_{rr}^d(s) + \sigma_{rr}^{ab}(s),$$

and rewrite Eqn 1 as

$$W_A = \int_{a_0}^{\infty} \sigma_{rr}^d(s) ds + \int_{a_0}^{\infty} \sigma_{rr}^{ab}(s) ds. \quad (2)$$

In the first approximation, we can write simply

$$W_A = \sigma_{ult}^d \cdot \lambda^d + \sigma_{ult}^{ab} \cdot \lambda^{ab}. \quad (3)$$

In Eqn 3, σ_{ult}^d and σ_{ult}^{ab} are maximum stresses due to only dispersion and only acid-base interaction, respectively. The λ^d value, the "effective range of action of dispersion forces", should be chosen so that the product $\sigma_{ult}^d \cdot \lambda^d$ is equal to the work against dispersion forces; in other words, the area of the rectangle in Fig. 3, a is equal to the area under the $\sigma_{rr}^d(s)$ plot. In similar way, λ^{ab} is defined. As can be seen from Eqn 3, to estimate the work of adhesion from a micromechanical test we must know four values, two components of adhesive pressure and two ranges of action of corresponding adhesion forces.

EXPERIMENTAL AND CALCULATION

Materials

Thermoplastic polymers — atactic polypropylene (PP), polystyrene (PS) and polycarbonate (PC) (all three polymers produced by BASF, Germany) were used as matrix materials. Untreated E-glass fibers, prepared at the Institute of Polymer Research, with a diameter of 14 μm were taken for the experiments.

Function $\sigma_{rr}(s)$ is very complicated and, generally speaking, unknown. However, we can make some reasonable assumptions about the behavior of this function and, in this way, simplify Eqn 1. As is known, there are two main types of adhesion forces, dispersion (London–van der Waals) forces and acid-base interactions. The dispersion interaction is universal, it exists between any two molecules and can act at relatively long distances, up to tens of nanometers. The acid-base interaction is due to local shift of electron density, and its range of action is limited to direct contact, i.e. not longer than several Ångströms (10^{-10} m). The intensity of the dispersion and acid-base interactions as a function of the distance between two surfaces is schematically shown in Fig. 3. It should be noted that in the propagating interfacial crack the action of these two types of forces are also separated in time (Fig. 4).

Samples

Specimens for micromechanical tests were prepared as follows. A small polymer particle was placed on a thin cover glass set up on a heated stage adjustable for temperature. The temperature of the glass surface was 200°C for PP, 230°C for PS, and 280°C for PC. After the particle has been melted down, a glass fiber was placed on the top of the droplet formed, and covered with a second glass plate. The specimen was kept in this state for about 2 minutes, which was sufficient for the droplet to flatten and for the fiber to immerse in the polymer. Then, the specimen was cooled down.

The finished specimen was a polymer disc (flattened droplet) having the diameter of 0.3–1.0 mm and thickness of about 0.15 mm, in which a glass fiber was embedded parallel to the disc face. All specimens were examined in a microscope, and those containing non-straight fibers or larger interfacial defects (e.g. air bubbles) were discarded.

Apparatus and experimental procedure

It is very important to accurately measure the value of the debond force, F_d . In recent years, a continuously monitored microbond (or pull-out) test has been proposed for this purpose [12, 13]. We used a mini tensile machine (Kammrath and Weiss GmbH, Germany) to produce

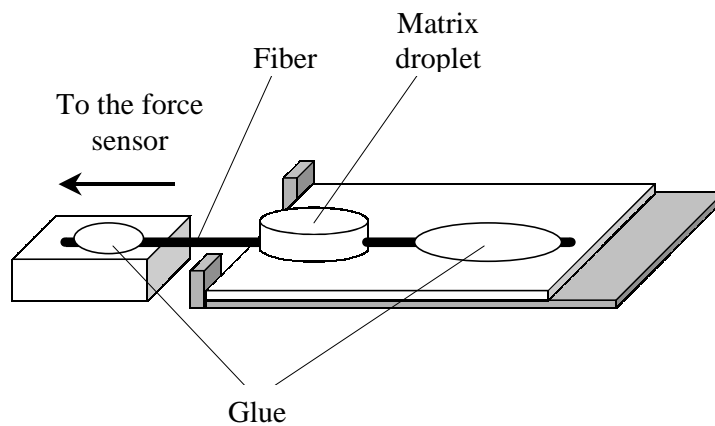


Fig. 5: Schematic view of the fiber-stretching test configuration

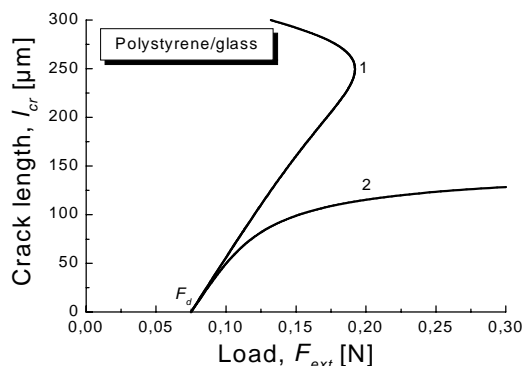


Fig. 6: Crack length as a function of external load. 1, microbond test; 2, fiber-stretching test

The testing device was placed on the stage of an optical microscope (Leica MZ12) equipped with a video camera connected to a computer, which made possible to record the picture of crack propagation in step with the applied load. Thus, the crack length, l_{cr} , was obtained as a

tensile load. The tested specimen was placed on a horizontal support glass plate clamped in the frame of the tensile machine, as shown in Fig. 5.

The experiment was performed in the following two versions:

1). (Microbond test). One glass plate was carefully separated from the polymer droplet. One fiber end was fixed, by a stiff cyano acrylate glue, on a metallic bar attached to the force sensor. The free fiber length was 0.2–2 mm.

2). (Fiber-stretching test, as we proposed in Ref. 14). Both glass plates were separated from the specimen. Then, one fiber end was glued to the metallic bar, and the other to the support glass plate (see Fig. 5). In this version of the test, the matrix disc could easily slide on the plate.

The testing speed was set to the minimum available with this tensile machine, 0.25 μm/s, to ensure slow crack propagation. The force applied to the fiber was recorded as a function of time.

function of the applied external force, F_{ext} . For the fiber-stretching test, the lengths of both cracks propagating from the ends of the matrix droplet were recorded.

Theoretical plots of the crack length as a function of applied load for the microbond and pull-out tests (as derived in Ref. 14) are shown in Fig. 6. An important result is that in both versions crack propagation was stable at the initial stage, and the crack length increased *linearly* with external load. This allows to determine the debond force, F_d , by linear fitting of the experimental plot $l_{cr}(F_{ext})$ and extrapolating the linear fit to zero crack length. This procedure is, in our opinion, much more accurate than simple visual detection of the crack initiation. It can be extremely difficult to discern visually between no crack and a very short crack; moreover, small interfacial flaws can influence the crack propagation. On the contrary, linear extrapolation gives reliable results which are well reproducible for long ($> 500 \mu\text{m}$) matrix droplets, when the F_d dependence on l_e ceases. It should be noted that our approach requires neither complete fiber pull-out nor short free fiber lengths; therefore, it is much more convenient than traditional microbond test. Its additional advantage is the possibility of handling large matrix droplets.

Calculation of the adhesive pressure

The adhesive pressure, σ_{ult} , was taken equal to the radial tensile stress, σ_{rr} , at the fiber-matrix interface at the point of fiber entry into the matrix for the moment of crack initiation ($F_{ext} = F_d$). For details see Scheer and Nairn [5]. Their equations for σ_{rr} in the fiber and in the matrix gave identical results, since at the interface this is the same interfacial normal stress.

Table 1: Work of adhesion and adhesive pressure for polymer/fiber systems

Fiber	Matrix	W_A^d [mJ/m ²]	W_A^{ab} [mJ/m ²]	W_A [mJ/m ²]	σ_{ult} [MPa]
Carbon T300	Nylon 6,6	76.2	17.1	93.3	132
E-glass	Nylon 6,6	61.9	46.9	108.8	208
E-glass	PS	70.1	42.0	112.1	193
E-glass	PP	65.8	1.5	67.3	99
E-glass	PE	68.0	0.0	68.0	81
E-glass	PC	69.9	41.7	92.2	277
E-glass	ABS	69.9	39.5	109.4	231

Using this approach, we have treated our own experimental data and the data from the literature on micromechanical tests with some fiber/polymer polymer composites, presented fully enough to calculate σ_{ult} . The calculated σ_{ult} values are presented in Table 1.

Calculation of the work of adhesion from inverse gas chromatography data

According to the Fowkes's theory [11], the thermodynamic reversible work of adhesion can be represented as a sum of the dispersion and acid-base components:

$$W_A = W_A^d + W_A^{ab}. \quad (4)$$

The contribution of dispersion forces is determined as doubled geometric mean of dispersion parts of free surface energies of the fiber (γ_f^d) and the matrix (γ_m^d):

$$W_A^d = 2\sqrt{\gamma_f^d \gamma_m^d}.$$

The acid-base term in Eqn 4 can be calculated as

$$W_A^{ab} = f \cdot n^{ab} \cdot (K_{Af} K_{Bm} + K_{Am} K_{Bf}),$$

where n^{ab} is the number of acid-base sites (possible donor-acceptor pairs) per unit interfacial area; K_A and K_B are coefficients characterizing respectively the acidity and the basicity of the surface (f is for the fiber and m is for the matrix), and f is a correcting factor (in agreement with Fowkes [11], it is taken equal to unity).

The values of acid-base parameters K_A and K_B can be determined using the inverse gas chromatography technique [8–10]. At present, these parameters are known for many polymers and fibers and can be found in the literature. We have calculated W_A^d and W_A^{ab} for the systems for which we were able to calculate σ_{ult} , either from our experiments or from the literature data (see Table 1).

RESULTS AND DISCUSSION

The observation of specimens under loading with a microscope showed that crack nucleation and further propagation was clearly discernible for all investigated polymers. The cracks always started at the points of fiber entry in the matrix. For the fiber-stretching test, they started nearly simultaneously from both ends and grew practically symmetrically towards the

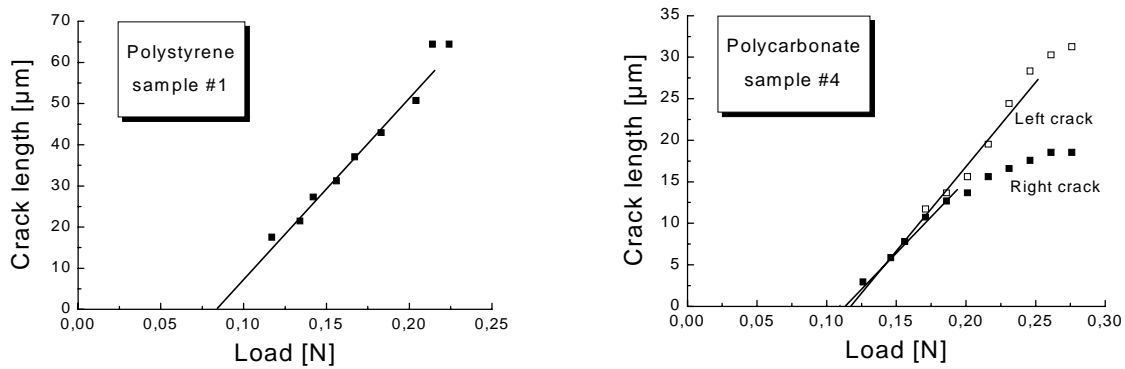


Fig. 7: Experimental relationships between the applied load and the crack length: the microbond test (a) and the fiber-stretching test (b)

middle of the sample. The crack propagation was stable and slow, which allowed to record the crack length for each specimen as a function of the applied load (Fig. 7). As can be seen from Fig. 7, initial parts of the $l_{cr}—F$ curves were linear for all systems, which is in good agreement with the theoretical considerations [14].

Table 1 shows the σ_{ult} values calculated, according to Scheer and Nairn, from experimental data for all investigated systems.

In Fig. 8, the adhesive pressure, σ_{ult} , in polymer/fiber systems is plotted as a function of the work of adhesion (determined by means of inverse gas chromatography) in these systems. As can be seen, this relationship is satisfactorily described by a linear function. However, there is no proportionality between the σ_{ult} and W_A values. This result might seem to run counter to fundamental physical principle, according to which the work of adhesion is a product of the force of adhesive pressure, acting at the interface, by a characteristic length corresponding to the range of action of this force:

$$W_A = \sigma_{ult} \cdot \lambda .$$

However, if we remember that W_A is a sum of works of two forces of different physical nature and having substantially different ranges of action (λ^d and λ^{ab}), the plot in Fig. 8 will look quite physical. Moreover, the obtained results allow estimation of λ^d and λ^{ab} values for polymer/fiber systems. From obvious equations

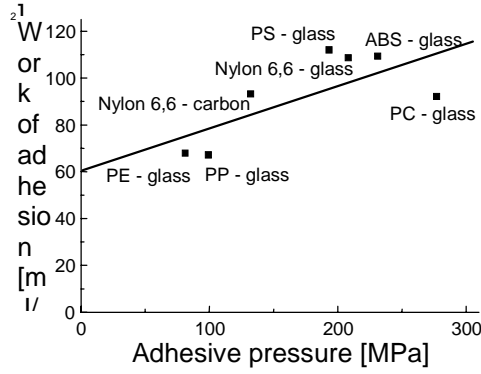


Fig. 8: Correlation between the adhesive pressure (from micromechanical tests) and the work of adhesion (from IGC data)

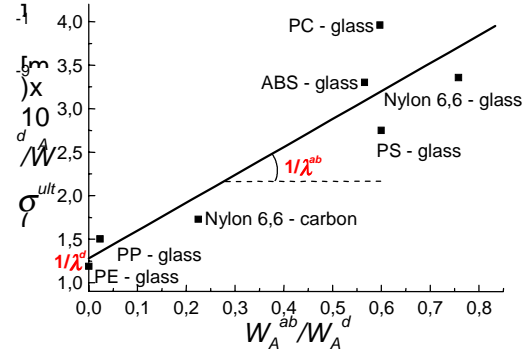


Fig. 9: Estimation of the ranges of action for dispersion and acid-base forces

$$\sigma_{ult} = \sigma_{ult}^d + \sigma_{ult}^{ab}$$

and

$$W_A = W_A^d + W_A^{ab}$$

we can easily deduce

$$\frac{\sigma_{ult}^d}{W_A^d} = \frac{\sigma_{ult}^d}{W_A^d} + \frac{\sigma_{ult}^{ab}}{W_A^d} = \frac{\sigma_{ult}^d}{\sigma_{ult}^d \cdot \lambda^d} + \frac{W_A^{ab} / \lambda^{ab}}{W_A^d} = \frac{1}{\lambda^d} + \frac{W_A^{ab} / W_A^d}{\lambda^{ab}}$$

Thus, having plotted σ_{ult}^d / W_A^d versus W_A^{ab} / W_A^d , we should obtain a straight line whose slope is equal to $1/\lambda^{ab}$ and the intercept on the vertical axis is $1/\lambda^d$. The converted plot is shown in Fig. 9. The characteristic range of action for the dispersion forces, from our data, appeared to be about 7.0 Å, which is of the order of the equilibrium intermolecular distance for the van der Waals interaction []. On the other hand, the value of $\lambda^{ab} \approx 3.2$ Å, obtained from Fig. 9, can be attributed to hydrogen bonds, whose formation is a typical result of acid-base interactions [15]. This result confirms physical validity of our model and suitability of adhesive pressure as a failure criterion.

CONCLUSION

Two new versions of micromechanical techniques have been developed: pulling a fiber out of very large matrix droplet and fiber loading at both ends (fiber-stretching test). On the one hand, these techniques are experimentally simple, they require neither very stiff testing equipment nor pull-out completion and can be used for testing various fiber-matrix systems. On the other hand, the newly proposed method of extrapolation of the crack-driving force to zero crack length allows to measure the debond force very accurately.

The adhesive pressure calculated from the measured debond force value can be used as a new interfacial failure criterion. For many fiber-matrix pairs, the adhesive pressure has been shown to be linearly dependent on the thermodynamic work of adhesion measured independently using the IGC technique.

REFERENCES

1. Désarmot, G. and Favre, J.-P., "Advances in Pull-Out Testing and Data Analysis", *Composites Science and Technology*, Vol. 42, 1991, pp. 151–187.
2. Gorbatkina, Yu. A., *Adhesive Strength of Fibre-Polymer Systems*, Ellis Horwood, New York, 1992.
3. Zhandarov, S. F. and Pisanova, E. V., "The Local Bond Strength and Its Determination by Fragmentation and Pull-Out Tests", *Composites Science and Technology*, Vol. 57, 1997, pp. 957–964.
4. Piggott, M. R., "Debonding and Friction at Fibre-Polymer Interfaces. I: Criteria for Failure and Sliding", *Composites Science and Technology*, Vol. 30, 1987, pp. 295–306.
5. Scheer, R. J. and Nairn, J. A., "A Comparison of Several Fracture Mechanics Methods for Measuring Interfacial Toughness with Microbond Tests", *Journal of Adhesion*, Vol. 53, 1995, pp. 45–68.
6. Marotzke, C., "Influence of the Fiber Length on the Stress Transfer from Glass and Carbon Fibers into a Thermoplastic Matrix in the Pull-Out Test", *Composite Interfaces*, Vol. 1, No. 2, 1993, pp. 153–166.
7. Piggott, M. R., "A New Model for Interface Failure in Fibre-Reinforced Polymers", *Composites Science and Technology*, Vol. 55, 1995, pp. 269–276.
8. Nardin, M. and Schultz, J., "Relationship between Fibre-Matrix Adhesion and the Interfacial Shear Strength in Polymer-Based Composites", *Composite Interfaces*, Vol. 1, No. 2, 1993, pp. 177–192.
9. Jacobasch, H.-J., Grundke, K., Uhlmann, P., Simon, F. and Mäder, E., "Comparison of Surface-Chemical Methods for Characterizing Carbon Fiber – Epoxy Resin Composites", *Composite Interfaces*, Vol. 3, No. 4, 1996, pp. 293–320.
10. Harding, P. H. and Berg, J. C., "The Role of Adhesion in the Mechanical Properties of Filled Polymer Composites", *Journal of Adhesion Science and Technology*, Vol. 11, 1997, pp. 471–473.
11. Fowkes, F. M., "Role of Acid-Base Interfacial Bonding in Adhesion", *Journal of Adhesion Science and Technology*, Vol. 1, No. 1, 1987, pp. 7–27.
12. Piggott, M. R. and Xiong, Y., "Direct Observation of Debonding in Fiber Pull-Out Specimens", *Fiber, Matrix, and Interface Properties*, ASTM STP 1290, Spragg, C. J. and Drzal, L. T., Eds., American Society for Testing and Materials, 1996, pp. 84–91.
13. Hampe, A. and Marotzke, C., "The Energy Release Rate of the Fiber/Polymer Matrix Interface: Measurement and Theoretical Analysis", *Journal of Reinforced Plastics and Composites*, Vol. 16, No. 4, 1997, pp. 341–352.
14. Zhandarov, S., Pisanova, E. and Schneider, K., "Fiber-Stretching Test: A New Technique for Characterizing Fiber-Matrix Interface Using Direct Observation of Crack Initiation and Propagation", *Journal of Adhesion Science and Technology*, 1999 (submitted).
15. Gutowski, W., "Thermodynamics of Adhesion", *Fundamentals of Adhesion*, Lee, L.-H., Ed., Plenum Press, New York, 1991, pp. 87–135.